Macromolecules

pubs.acs.org/Macromolecules Article

Inverse Miniemulsion Photoiniferter Polymerization for the Synthesis of Ultrahigh Molecular Weight Polymers

Rebecca A. Olson, Megan E. Lott, John B. Garrison, Cullen L. G. Davidson, IV, Lucca Trachsel, Diego I. Pedro, W. Gregory Sawyer, and Brent S. Sumerlin*

Cite This: *Macromolecules* 2022, 55, 8451−8460 Read Online

ACCESS | Metrics & More | Article Recommendations | Supporting Information

ABSTRACT: We describe the synthesis of ultrahigh molecular weight water-soluble polymers *via* photoiniferter polymerization under inverse miniemulsion conditions. The catalyst-free heterogeneous process is mediated using low-intensity UV irradiation and offers rapid polymerization rates, excellent molecular weight control, polymer end-group fidelity, temporal control, advanced architectures, and most notably, viscosity control. We refined the polymerization conditions by considering the nature of the surfactant, costabilizer, and iniferter agent to achieve acrylamido homopolymers and block copolymers of molecular weights exceeding 1,000,000 Da at ambient temperature. This approach to well-defined ultrahigh molecular weight polymers overcomes the complications of high viscosity to facilitate eventual scale-up.

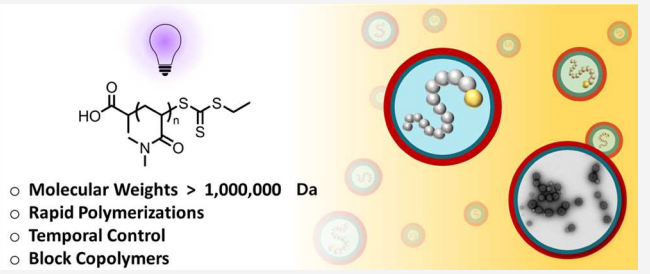

INTRODUCTION

Heterogeneous polymerization systems comprise approximately one-fifth of worldwide polymer production processes.[1−3] The prevalence of heterogeneous polymerizations arises from the advantages of viscosity control, improved heat transfer, high polymerization rates, and the ability to produce high molecular weight polymers.[3,4] These benefits largely result from the dispersion of insoluble monomers in stabilized droplets within a continuous phase where polymerization occurs in the locus of the droplets and the continuous phase acts as a heat sink for the exothermic polymerization. Importantly, the viscosity of the emulsion is approximately that of the continuous phase and is not significantly affected by the molecular weight of the growing polymer, unlike bulk and solution polymerization systems.

Heterogeneous polymerizations exhibit unique kinetics and rapid polymerization rates and remain an active area of study.[1,4−16] Miniemulsion polymerizations are of particular interest due to their enhanced colloidal stability and more uniform droplet size and composition, attributes associated with improved control of many living polymerization systems.[9,17−20] Within miniemulsions, smaller particles of monomers are formed initially and serve as the loci of polymerization. Strong shearing is generally necessary to generate the high energy interfaces of the 50−500 nm-diameter particles.[17,21] Thus, the interfaces must be stabilized with surfactants and, often, costabilizers, which limit particle coalescence and monomer diffusion between droplets.[21] This approach has allowed miniemulsion monomer droplets to serve as nanoreactors for reversible-deactivation radical polymerization (RDRP), *e.g.*, reversible addition−fragmentation chain-transfer (RAFT) polymerization, atom transfer radical polymerization (ATRP), and nitroxide-mediated polymerization (NMP), among others.[9,17,22−27] Of note, the enhanced polymerization rate and limited termination within these nanoreactors facilitate the formation of controlled ultrahigh molecular weight polymers,[20,28] which remains a challenge and focus for synthetic polymer chemists.[29−38,64]

Photoiniferter polymerization is an additional RDRP technique that we have employed to synthesize well-controlled ultrahigh molecular weight (UHMW) polymers exceeding 1,000,000 Da.[30,31] Specific reagents that can serve as initiators, transfer agents, and terminators have been coined iniferters and were initially explored for the synthesis of controlled polymers by Otsu in the early 1980s.[39,40] Thiocarbonylthio photoiniferters of the basic structure ZC(═S)SR undergo homolytic bond photolysis upon irradiation with visible or UV light to generate two radicals: one that can initiate polymerization (R•) and another that serves as a stable radical capable of reversible termination (Z(C═S)S•) to yield thiocarbonylthio end groups that permit degenerative chain transfer (Scheme 1).[41−47] These polymerizations require no exogenous initiator beyond the photoiniferter. Temporal control is also

Received: June 14, 2022
Revised: August 29, 2022
Published: September 22, 2022

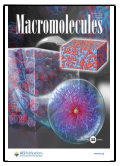

https://doi.org/10.1021/acs.macromol.2c01239
Macromolecules 2022, 55, 8451−8460

Scheme 1. (A) Photolytic Bond Cleavage of a Generic Photoiniferter (ZC(═S)SR) and (B) Photoiniferter Polymerization of *N,N*-Dimethylacrylamide (DMA) using 2-(Ethylthiocarbonothioylthio)propanoic Acid (iniferter 1) to Produce Poly(*N,N*-dimethylacrylamide) (PDMA)

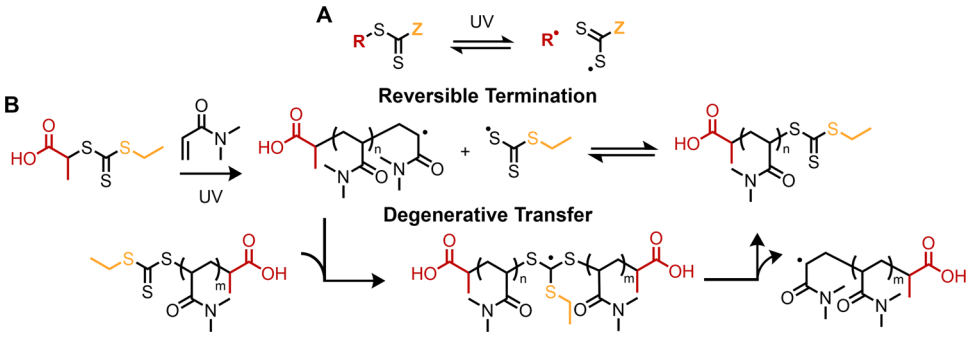

imparted to these systems with the simple tuning of light intensity.

Evidence suggests that both reversible termination and degenerative transfer processes are important for control during photoiniferter polymerization, where the predominant mechanism varies based on the structure of the iniferter.[31,48,49] Judicious choice of conditions (*i.e.*, high k_p monomers, appropriate solvents, high monomer concentration, high viscosity, and no exogenous initiator) allows an unprecedented opportunity to increase the ratio of the rate of polymerization (R_p) to the rate of termination (R_t) to favor the formation of ultrahigh molecular weight species.[30,31,37,50,51] In particular, high viscosity, which is a consequence of the synthesis of the ultrahigh molecular weight polymers, helps suppress the rate of diffusion-controlled bimolecular reactions such as termination, and has been shown to be an important factor when targeting well-defined polymers of ultrahigh molecular weights (10^5–10^7 Da). Unfortunately, the extremely high viscosities that enable access to such chain lengths may limit the eventual scale-up of such an approach. Photoiniferter polymerization has seen very limited exploration in (mini)emulsion systems,[25,52−55] but given the benefits of the latter, where high viscosity is limited to the nanoscale reaction particles, we reasoned that such an approach may have significant potential for the scalable synthesis of ultrahigh molecular weight polymers.

Here, we present the use of photoiniferter polymerization for the formation of well-controlled UHMW polymers under inverse miniemulsion conditions. The use of a heterogeneous system limits the viscosity of the overall mixture while simultaneously helping mitigate the polymerization exotherm. Translation of photoiniferter polymerization into a miniemulsion system serves as a significant step toward making this approach to UHMW polymers scalable and more industrially relevant, potentially facilitating their utility in a number of fields, including the production of flocculants, coacervates, protein mimetics, photonic materials, and elastomers.[35,37,46,56−58]

RESULTS AND DISCUSSION

Initially, we sought to explore the effect of various experimental conditions for the synthesis of UHMW (>10^6 Da) poly(*N,N*-dimethylacrylamide) (PDMA) using photoiniferter polymerization under inverse miniemulsion conditions at ambient temperature (Figure 1). We selected reaction components that had low UV cutoffs to limit absorption and maximize the photolysis kinetics of the iniferter. Moreover, it was critical to select a thiocarbonylthio iniferter with suitable water solubility

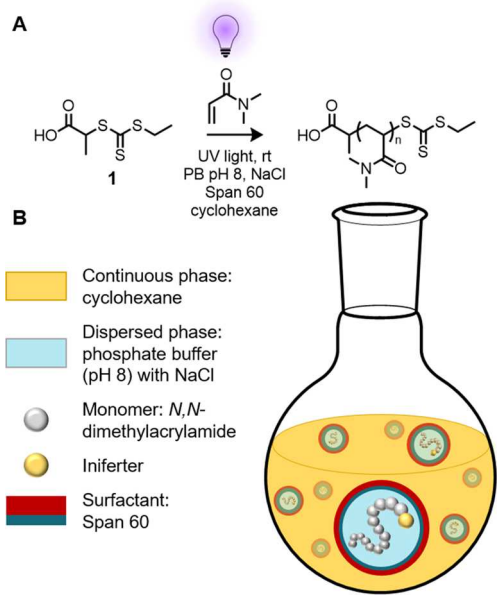

Figure 1. (A) Photoiniferter polymerization scheme of DMA using iniferter **1** under inverse miniemulsion conditions. (B) Representation of the inverse miniemulsion polymerization components.

and reactivity to remain within the aqueous phase to effectively mediate polymerization. We also sought to identify surfactants and costabilizers that would afford stable particles on the order of ∼150 nm in diameter, which allowed access to UHMW polymers with controlled chain lengths and dispersities, chain-end fidelity, and the on/off temporal control associated with photopolymerization.

Our initial goal was the formation of a miniemulsion with stable aqueous droplets dispersed in a continuous organic phase that would serve as nanoreactors for the polymerization of *N,N*-dimethylacrylamide (DMA). Cyclohexane was chosen as the continuous organic phase due to its immiscibility with water and low UV absorbance. The dispersed phase consisted of phosphate buffer (PB, pH = 8), DMA, 2-(ethylthiocarbonothioylthio)propanoic acid (iniferter **1**), and the internal standard *N,N*-dimethylformamide (DMF) to allow determination of monomer conversion *via* ^{1}H NMR spectroscopy. Initially, a [DMA]:[iniferter] ratio of 10,000:1 was chosen, where [DMA] = 5 M within the aqueous phase, to target well-defined polymers of ∼1,000,000 Da (Figure 1A and Figures S1 and S2). The miniemulsions were formed by sonicating the reaction components for 15 min.

https://doi.org/10.1021/acs.macromol.2c01239
Macromolecules 2022, 55, 8451−8460

Sorbitan monostearate (Span 60) was employed as the surfactant for droplet size and stability studies, as it is a common surfactant for traditional oil-in-water emulsions. Span 60 possesses a large 17-carbon hydrophobic tail coupled to a small hydrophilic sorbitan head and contains no unsaturated bonds or UV chromophores that might otherwise interfere with the polymerization. Surfactant loadings of 5, 7.5, 10, 12.5, and 15 wt % (relative to the dispersed phase) were tested for particle size and stability over 18 h of UV irradiation (Table S1). The particle size was monitored by dynamic light scattering (DLS), revealing particles with diameters of 120−140 nm across the surfactant loading range. However, significant macroscopic precipitation occurred during polymerization at the lower concentrations of 5 and 7.5 wt % surfactant loadings (Figure S3). Very minor precipitation was visible with 10 and 12.5 wt % surfactant loadings, and there was no significant precipitation with a surfactant load of 15 wt % (Figure S3). Span 60 was also blended with another surfactant, Tween 60, in an attempt to improve the particle stability (Table S2). However, the addition of Tween 60, which has a larger hydrophilic component, resulted in decreased particle stability as evidenced by an initial increase in size by DLS and eventual macroscopic phase separation. Sodium chloride was also introduced to the system as a costabilizer to limit particle destabilization *via* Ostwald ripening (Table S3).[21] NaCl was observed to enhance the stability of the particles as seen through decreased droplet dispersity *via* DLS early in the polymerization. A sample polymerization with the optimized salt and surfactant equivalents are shown in Table 1.

Table 1. Conditions for Optimized Inverse Miniemulsion Polymerization of DMA at 30 °C and 1000 RPM Stir Rate

phase	reaction component	molar equivalents	weight percent[a]	mass (mg)
dispersed (aqueous)	DMA	10,000		500
	iniferter	1		0.106
	PB (pH 8)			500
	NaCl		6	60
	DMF			106
surfactant	Span 60		15	150
continuous (organic)	cyclohexane			10,000

[a]Weight percent with respect to the total mass of the monomer and water in the dispersed phase.

As seen in Figure 2A, the unreacted emulsion was optically clear after sonication (Figure 2A). Mixture clarity is dependent on the nanoscale droplet size in the system (Figure 2B−D), limited solid content, and similar refractive indices of cyclohexane and the 5 M DMA dispersed phase.[1,59] Reducing the dispersed phase DMA concentration from 5 to 2 M resulted in an opaque mixture despite a small droplet size and identical mass ratio of the dispersed phase to the continuous phase (Figure S4). The 2 M polymerization still proceeded readily. Particle destabilization was observed at monomer concentrations above 5 M.

The particle size of the inverse miniemulsion system was investigated using transmission electron microscopy (TEM) (Figure 2C,D, Scheme S1, and Figures S5 and S6). To ensure particle stability during drop casting and imaging, the crosslinker *N*-methylenebisacrylamide (MBA) was included in a model polymerization at a concentration of 8 mol % relative to DMA. The crosslinker resulted in stable polymer particles amenable to TEM sample preparation. The number-average diameter (d_N) determined by TEM was 78 nm, which was in relatively good agreement with the d_N determined by DLS of 85 nm.

Ultrahigh molecular weight polymers of ∼1,000,000 Da could be synthesized using iniferter **1** under the optimized inverse miniemulsion conditions (Figure 3A, Table S4, and Figure S7). Size exclusion chromatography (SEC) data suggested that the synthesis of higher molecular weight polymers was more challenging, potentially attributed to chain transfer reactions, presumably with a surfactant (Table S5 and Figure S8). Notably, a polymer with a molecular weight of 1,210,000 Da was accessible by reducing the temperature from 30 to 10 °C, an observation potentially consistent with the occurrence of chain transfer. For all polymerizations, the global viscosity of the system remained low, and the mixtures were easily stirred with a magnetic stir bar (Figure 3B). As a comparison, the homogeneous aqueous polymerization of DMA in PB (pH 8), with conditions mimicking the dispersed phase of the miniemulsion, produced a high-viscosity solution due to the high concentration of the UHMW PDMA (Figure 3C).

To gain further insight into the controlled nature of this heterogeneous polymerization approach, polymerizations mediated with iniferter **1** were investigated in more detail (Figure 4). For a polymerization targeting a molecular weight

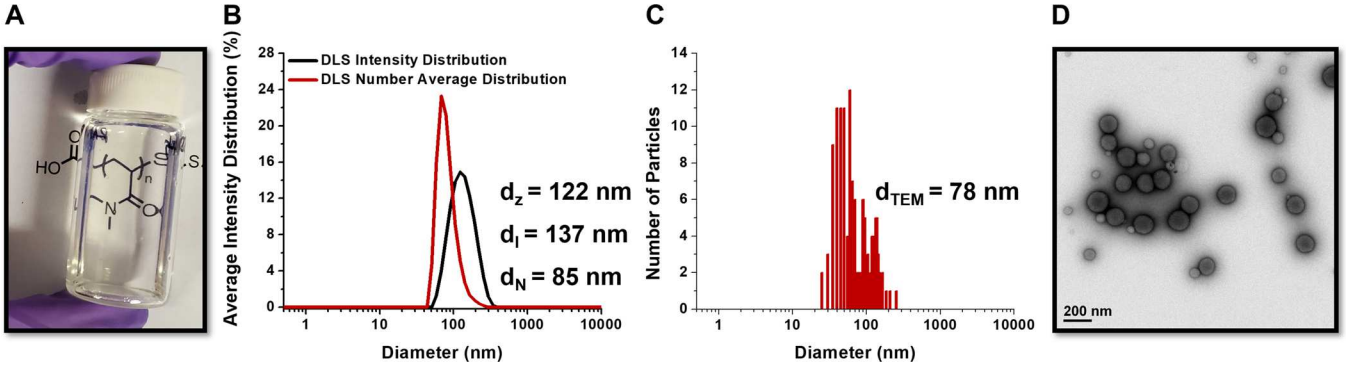

Figure 2. (A) Photo of an emulsion formulated as described in Table 1 taken after sonication and prior to polymerization. (B) DLS size distributions showing the number-average (d_N), intensity-average (d_I), and *z*-average (d_z) hydrodynamic diameters of the particles after polymerization in the presence of MBA as a crosslinker. (C) Size distribution of crosslinked PDMA particles (n = 133) from TEM images. (D) TEM image of PDMA particles with an MBA crosslinker.

https://doi.org/10.1021/acs.macromol.2c01239
Macromolecules 2022, 55, 8451−8460

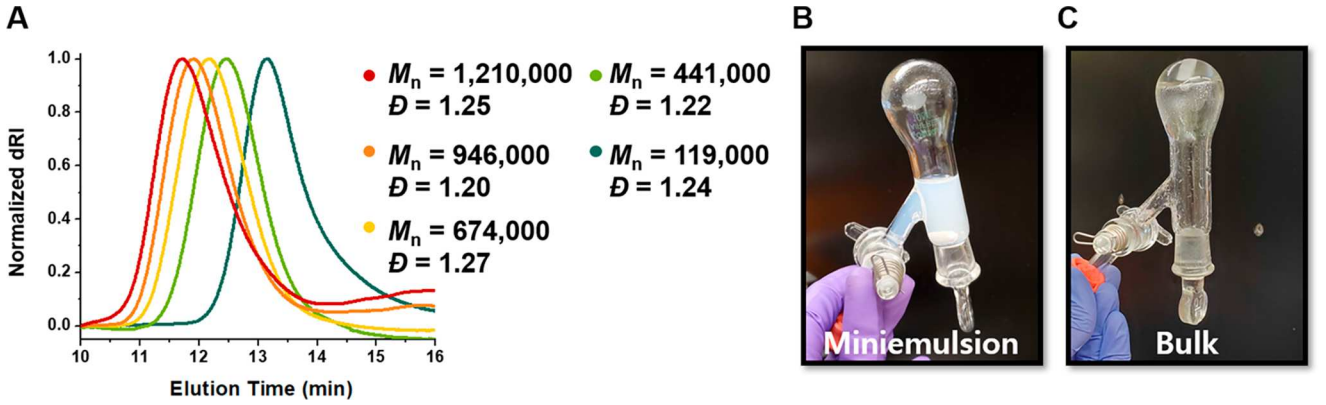

Figure 3. (A) SEC traces of PDMA prepared by inverse miniemulsion photoiniferter polymerization with molecular weights ranging from 119,000 to 1,210,000 Da. The polymer reaching a molecular weight of 1,210,000 Da (red trace) was accessible by reducing the polymerization temperature to 10 °C. (B) Photo of a postpolymerization DMA miniemulsion system in a 10 mL Schlenk flask. Upon inversion, the mixture readily flows. (C) Photo of a postpolymerization DMA polymerization in homogeneous aqueous media (5 M DMA in PB) in a 10 mL Schlenk flask. Upon inversion, the high-viscosity solution flows very slowly.

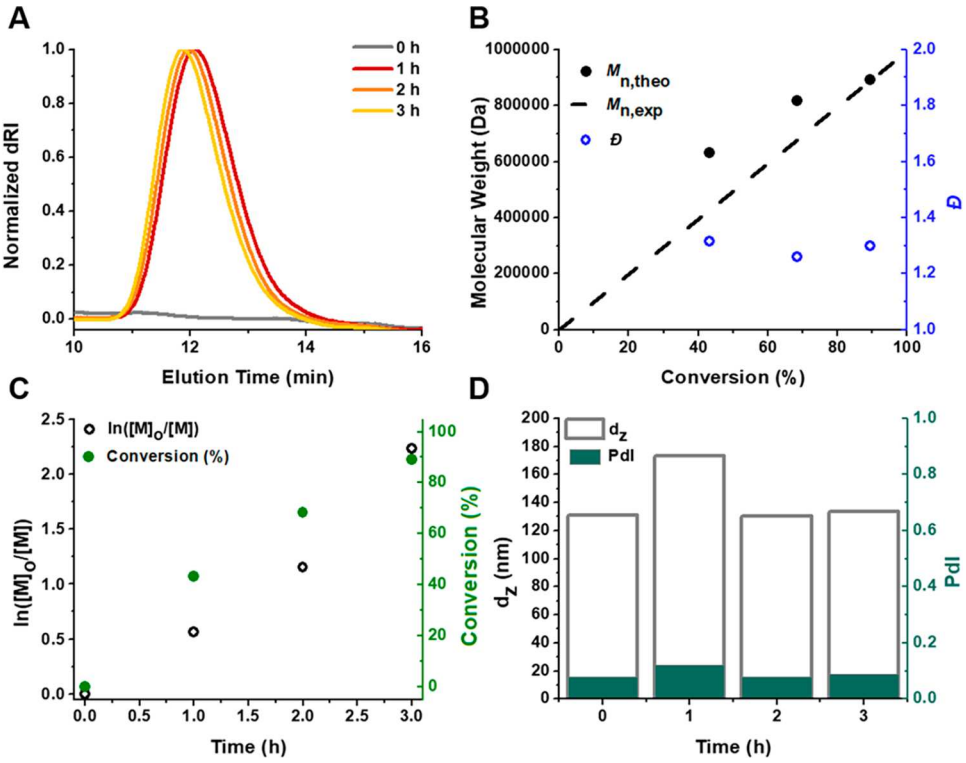

Figure 4. (A) SEC traces of DMA polymerization mediated by iniferter **1** with conditions as listed in Table 1, showing a shift to lower elution times with increased polymerization time. (B) Experimental and theoretical number-average molecular weight (M_n) and molar mass dispersity as a function of monomer conversion. (C) Linear pseudo-first-order kinetic plot indicating a constant radical flux in the system. (D) Particle diameter (d_z) plotted as a function of polymerization time.

of 1,000,000 Da at complete conversion, the experimental number-average molecular weight increased as a function of conversion and the dispersity remained reasonable ($Đ < 1.4$) throughout the polymerization (Figure 4A,B). Additionally, the linear pseudo-first-order kinetic plot indicated that the radical concentration remained constant up to high monomer conversion (Figure 4C). DLS analysis revealed that the particle diameter did not change appreciably during the polymerization (Figure 4D), as expected for miniemulsion systems, although a slight (and reversible) increase in particle size was consistently observed at lower conversions.

Photoiniferter polymerizations are controlled by a combination of reversible termination and degenerative chain transfer,[31,48,49] and consideration must be given when selecting an iniferter for a given set of polymerization conditions. Accordingly, we explored other iniferters to determine the effect on polymerization control under inverse miniemulsion conditions (Figure 5A,B and Figures S11−S15). For an iniferter to effectively initiate and mediate polymerization in an aqueous medium, it must be stable to hydrolysis and have water solubility sufficient for effective partitioning into the locus of polymerization, *i.e.*, the water- and monomer-containing droplet.[17,60,61]

https://doi.org/10.1021/acs.macromol.2c01239
Macromolecules 2022, 55, 8451−8460

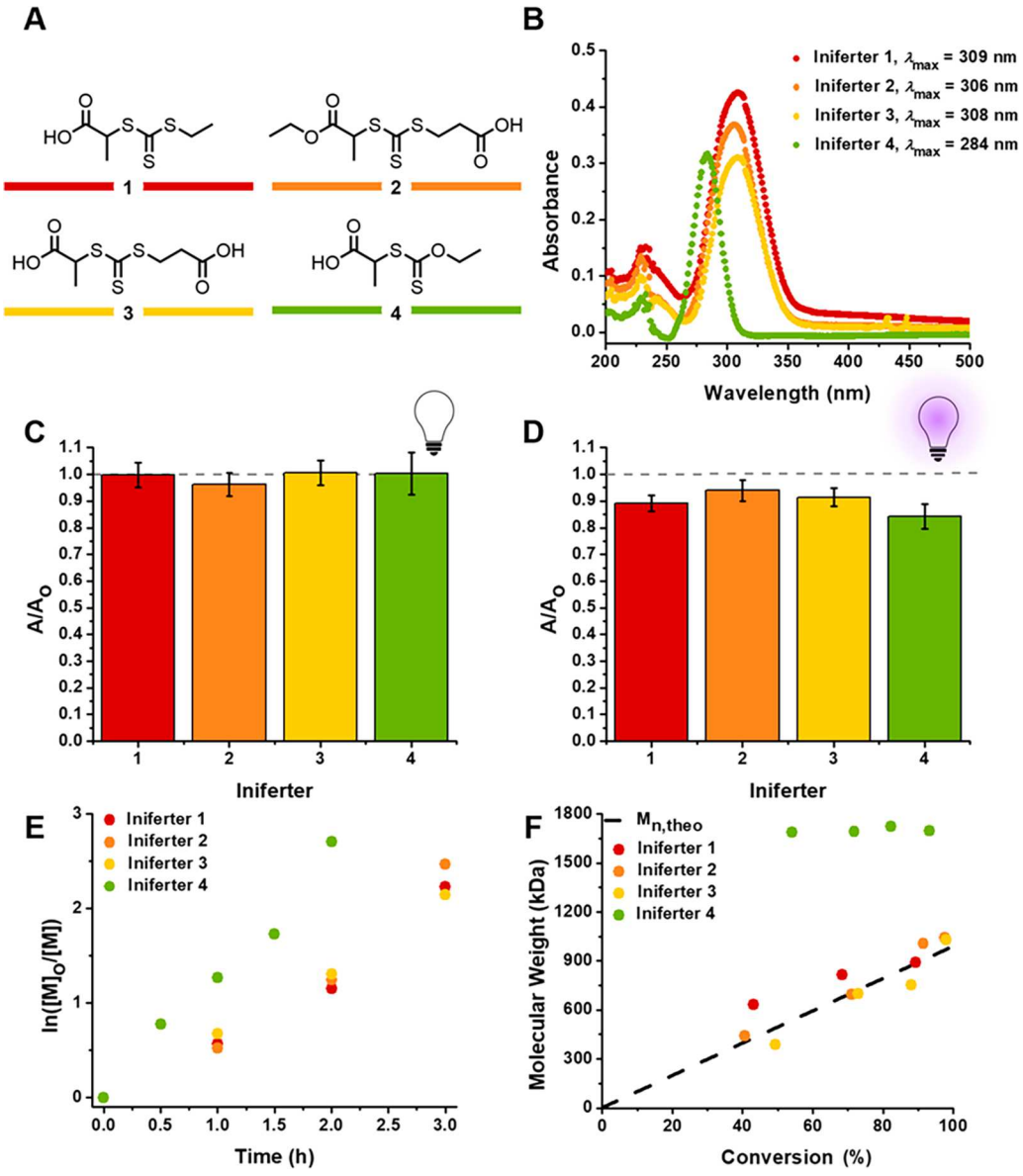

Figure 5. (A) Structures of iniferters **1**−**4**. (B) UV−vis absorbance spectra and λ_{max} absorbance of iniferters **1**−**4**. (C) Change in the UV absorbance of iniferters **1**−**4** in PB before and after the addition of cyclohexane without UV light. (D) Change in the UV absorbance of iniferters **1**−**4** in PB after UV irradiation. (E) Pseudo-first-order kinetic plots and (F) Experimental molecular weight (M_n) plotted as a function of monomer conversion for polymerizations carried out using iniferters **1**−**4**.

The hydrolytic stability of iniferters **1**−**4** (Figure 5A) was monitored using UV−vis spectroscopy, as the hydrolysis of the trithiocarbonate would have deleterious effects on polymerization control (Figure S16).[17,62,63] The UV absorption spectra and molar extinction coefficients were determined for each iniferter in PB (Figure S15). Iniferters **1**−**4** were dissolved in PB and monitored by UV−vis spectroscopy for 18 h, during which time there was no change in the UV absorbance of iniferters **1**, **2**, or **4**; however, iniferter **3** demonstrated a slight decrease in absorbance, which could result from hydrolysis (Figure S16).[62,63] The partitioning behavior of the iniferters in water/cyclohexane mixtures was monitored by UV−vis spectroscopy (Figure 5C,D and Figures S17 and S18). The UV absorbances of iniferters **1**−**4** in PB were measured before and after the introduction of cyclohexane at concentrations relevant to polymerization conditions. In the absence of UV irradiation (mimicking the polymerization system prior to initiation), the UV absorbance of the iniferters did not change appreciably upon addition and mixing with cyclohexane. These results suggest that the iniferters favorably partition in the aqueous phase (Figure 5C and Figure S17). When the biphasic reaction mixtures were subjected to UV irradiation (mimicking the polymerization system upon initiation), all iniferters showed a decrease in absorbance intensity within the aqueous phase, indicating either loss of the intact iniferter or a reduction in the concentration of the thiocarbonylthio fragment of the iniferter after homolytic bond cleavage (Figure 5D and Figure S18). Interestingly, iniferters **2** and **3** exhibited slightly smaller decreases in absorbance intensity under UV irradiation, likely due to their carboxylate-containing Z groups, which could suggest that sulfur-centered thiocarbonylthiyl radicals with polar substituents are more likely to remain within the aqueous locus of polymerization after C−S bond cleavage by photolysis.

https://doi.org/10.1021/acs.macromol.2c01239
Macromolecules 2022, 55, 8451−8460

Table 2. Inverse Miniemulsion Photoiniferter Polymerizations Conducted with Iniferter 3[h]

target MW (Da)	[DMA]:[iniferter]	temp[a] (°C)	conv.[b] (%)	$M_{n,theo}$[c] (Da)	$M_{n,exp}$[d] (Da)	$Đ$[e]	$d_{z,prior}$[f] (nm)/PDI	$d_{z,after}$[g] (nm)/PDI
1,000,000	10,000:1	30	93	918,000	1,030,000	1.23	130/0.10	150/0.08
2,000,000	20,000:1	30	>95	1,980,000	1,250,000	1.36	148/0.06	135/0.12
5,000,000	50,000:1	30	>95	4,960,000	1,550,000	1.35	125/0.16	119/1.15
10,000,000	100,000:1	30	>95	9,910,000	1,920,000	1.24	148/0.09	131/0.10
1,000,000	10,000:1	10	>95	992,000	1,290,000	1.32	152/0.10	130/0.13
2,000,000	20,000:1	10	>95	1,980,000	1,400,000	1.33	142/0.08	141/0.11
5,000,000	50,000:1	10	>95	4,960,000	1,720,000	1.22	146/0.11	124/0.12
10,000,000	100,000:1	10	>95	9,910,000	1,862,000	1.26	133/0.09	142/0.08

[a]Polymerization temperature. [b]Monomer conversion determined by ^{1}H NMR spectroscopy. [c]Theoretical number-average molecular weight. [d]Experimental number-average molecular weight determined by SEC. [e]Final polymer chain dispersity. [f]Hydrodynamic diameter of the inverse miniemulsion particles prior to polymerization, as determined by DLS. [g]Hydrodynamic diameter of the inverse miniemulsion particles after polymerization, as determined by DLS. [h]All polymerizations were conducted for 12 h.

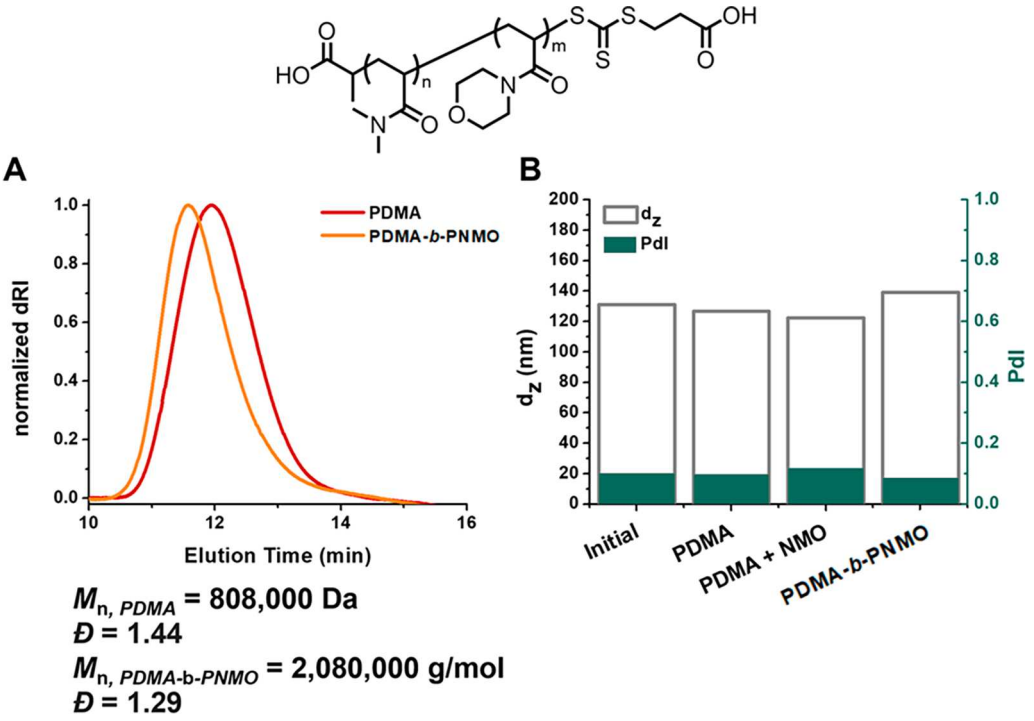

Figure 6. (A) SEC traces of PDMA and PDMA-*b*-PNMO mediated by iniferter **3** under the conditions indicated in Table 1. PDMA prepared by inverse miniemulsion polymerization ($M_{n,exp}$ = 808,000 Da, $M_{n,theo}$ = 880,000 Da, and $Đ$ = 1.44) was chain-extended with NMO to a final conversion of ∼99% in 4 h ($M_{n,exp}$ = 2,080,000, $M_{n,theo}$ = 2,480,000, and $Đ$ = 1.29). (B) *Z*-average particle diameters (d_z) before the initial polymerization, after DMA polymerization, after the NMO/PB solution was added to the PDMA miniemulsion, and after PDMA-*b*-PNMO synthesis.

The rate of the photoiniferter polymerizations was predominately dictated by the nature of the light-absorbing thiocarbonylthio moiety within the photoiniferter, namely, the trithiocarbonate (**1**−**3**) or the xanthate (**4**) (Figure 5E). The water-soluble trithiocarbonates **1**−**3** resulted in polymerizations with similar rates (Figure 5E) and allowed the synthesis of ultrahigh molecular weight polymers in a controlled manner (Figures 4 and 5F and Figures S19 and S20), as evidenced by the number-average molecular weight of the polymers increasing linearly with monomer conversion and relatively narrow molecular weight distributions being observed *via* SEC. Iniferter **3**, which contains carboxyl groups on both its R and Z groups that enhance solubility in the aqueous phase, resulted in the best combination of polymerization control and access to molecular weights in the range of 10^6 Da (Table 2). The enhanced solubility of the thiocarbonylthio Z group of iniferter **3** in the locus of the polymerization potentially helped limit loss to the organic phase of the thiocarbonylthiyl radicals that result from photolysis. Nevertheless, polymerization control was diminished when targeting M_n values greater than 2×10^6 Da. Given that we have previously observed trithiocarbonates of this type to provide access to PDMA with M_n approaching 5×10^6 Da when conducted in homogeneous aqueous media, this observation may again suggest complications such as reduced chain-end fidelity arising from chain transfer to the surfactant (Figure S9), although carrying out the polymerizations at a reduced temperature of 10 °C did not result in significantly improved control in this case.

Iniferter **4**, a hydrophilic xanthate, failed to allow controlled polymerization, as evidenced by an unchanged M_n with increasing conversion (Figure 5F and Figure S21). Xanthates

https://doi.org/10.1021/acs.macromol.2c01239
Macromolecules 2022, 55, 8451−8460

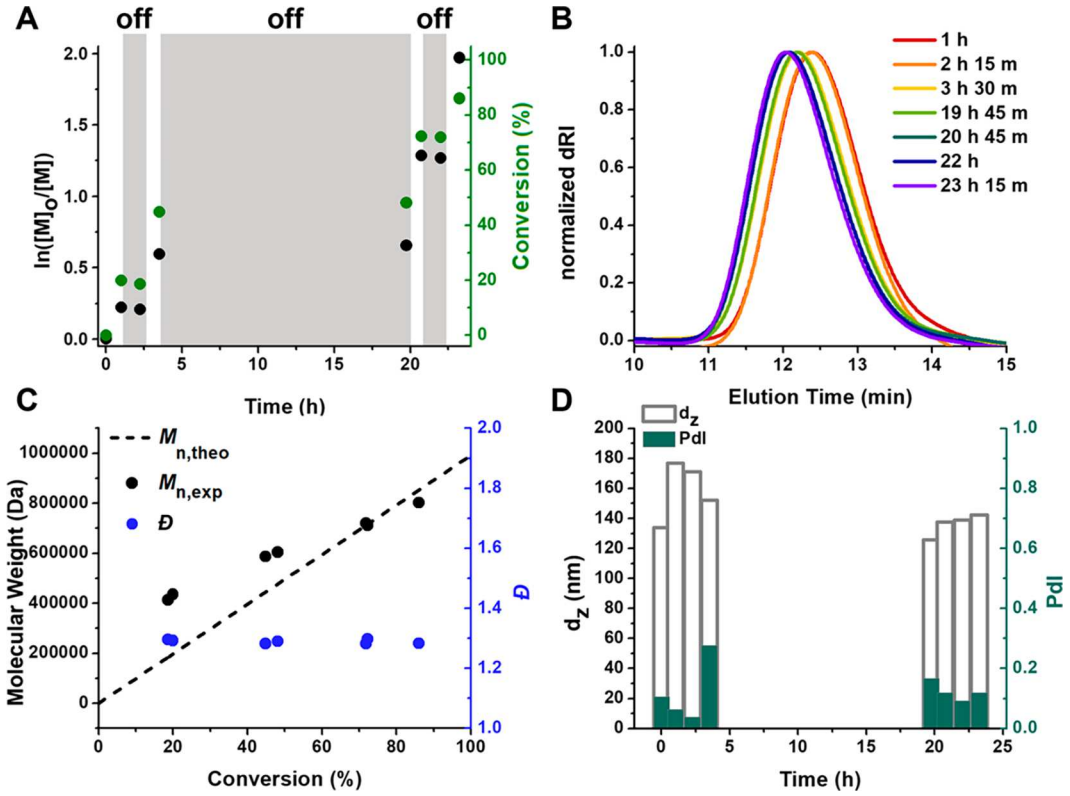

Figure 7. Temporal control studies of DMA polymerization using iniferter **1** under the inverse miniemulsion conditions of Table 1. (A) Pseudo-first-order kinetic plot and monomer conversion with time during on−off light cycles. (B) SEC traces showing that the molecular weight increases with increasing monomer conversion. (C) Experimental molecular weight and dispersity plotted as a function of monomer conversion. $M_{n,exp}$ increases linearly with monomer conversion, and dispersities remain reasonable throughout the polymerization. (D) Particle size plotted as a function of polymerization time throughout the on−off light cycles.

undergo rapid photoexcitation and photolysis, and previous work has shown that they can be used as an iniferter to efficiently form UHMW polymers in a controlled manner.[31] However, xanthates have a relatively low chain transfer constant to PDMA, suggesting that reversible termination plays a more significant role in deactivation than when DMA polymerizations are mediated with a trithiocarbonate iniferter.[31,48] The loss of control in miniemulsion conditions may suggest that partitioning of the thiocarbonylthiyl radical of iniferter **4** into the organic phase may compromise the effectiveness of reversible termination.

The inverse miniemulsion polymerizations of DMA mediated with trithiocarbonate iniferters **1** and **3** were well controlled, as evidenced by the polymerization kinetics (Figures 4 and 5), and were expected to produce polymers with reasonable end-group fidelity despite the possibility of chain transfer. To verify chain-end retention during the inverse miniemulsion conditions, PDMA prepared with iniferters **1** and **3** was chain-extended *in situ* with additional DMA or 4-acryloyl morpholine (NMO) to synthesize a second block with a target molecular weight of 1,000,000 Da (Figure 6 and Figures S22−S24). These block copolymerizations were carried out in a one-pot manner, wherein a solution of the second monomer in PB was added to the system when the initial PDMA homopolymer synthesis had reached ∼85+% monomer conversion. DLS indicated that the polymer particles swelled with the addition of the solvent and monomer. SEC traces of the original PDMA cleanly shifted to higher molecular weights during the addition of the second block, suggesting good chain-end retention.

Finally, we illustrate the scale-up potential using similar inverse miniemulsion polymerization conditions, targeting 5 g of PDMA (Table S6 and Figure S25), and we demonstrate that the temporal control typical of photopolymerizations was imparted to this inverse miniemulsion polymerization system (Figure 7). Photoexcitation of the iniferter and radical formation only occurred when the light source was on. For the polymerization of DMA mediated by iniferter **1** under the conditions described in Table 1, little to no monomer conversion was observed when the light was off, and the molecular weight increased only with increasing conversion during irradiation (Figure 7A,C). Throughout the on−off light cycles, the particle size was constant, suggesting that the polymerization particles remained stable over 16 h in the dark (Figure 7D).

■ CONCLUSIONS

The inverse miniemulsion system we designed serves as a model for the synthesis of well-controlled UHMW PDMA by photoiniferter polymerization. The influence of reaction parameters such as surfactant loading, salt concentration, and iniferter identity all played important roles in controlling the droplet size and enhancing molecular weight control. The appropriate choice of miniemulsion components enabled the rapid synthesis of PDMA with a molecular weight exceeding 1,000,000 Da in a mixture, which maintained a low viscosity. UHMW polymers retained a reasonable degree of chain-end fidelity evidenced by *in situ* chain extension that generated UHMW block copolymers without intermediate purification.

https://doi.org/10.1021/acs.macromol.2c01239
Macromolecules 2022, 55, 8451−8460

Overall, the use of photoiniferter polymerization in a miniemulsion system is an important step to scalable production of UHMW materials with controlled molecular weight, chain-end retention, and complex architectures. Ongoing work in our lab is focused on increasing the range of molecular weights that can be accessed by this approach.

■ ASSOCIATED CONTENT

Supporting Information

The Supporting Information is available free of charge at https://pubs.acs.org/doi/10.1021/acs.macromol.2c01239.

Synthetic protocols, polymerization methods, and additional supporting figures (PDF)

■ AUTHOR INFORMATION

Corresponding Author

Brent S. Sumerlin − *George & Josephine Butler Polymer Research Laboratory, Center for Macromolecular Science & Engineering, Department of Chemistry, University of Florida, Gainesville, Florida 32611-7200, United States;* orcid.org/0000-0001-5749-5444; Email: sumerlin@chem.ufl.edu

Authors

Rebecca A. Olson − *George & Josephine Butler Polymer Research Laboratory, Center for Macromolecular Science & Engineering, Department of Chemistry, University of Florida, Gainesville, Florida 32611-7200, United States*

Megan E. Lott − *George & Josephine Butler Polymer Research Laboratory, Center for Macromolecular Science & Engineering, Department of Chemistry, University of Florida, Gainesville, Florida 32611-7200, United States;* orcid.org/0000-0001-9854-6252

John B. Garrison − *George & Josephine Butler Polymer Research Laboratory, Center for Macromolecular Science & Engineering, Department of Chemistry, University of Florida, Gainesville, Florida 32611-7200, United States*

Cullen L. G. Davidson, IV − *George & Josephine Butler Polymer Research Laboratory, Center for Macromolecular Science & Engineering, Department of Chemistry, University of Florida, Gainesville, Florida 32611-7200, United States*

Lucca Trachsel − *George & Josephine Butler Polymer Research Laboratory, Center for Macromolecular Science & Engineering, Department of Chemistry, University of Florida, Gainesville, Florida 32611-7200, United States;* orcid.org/0000-0002-4342-1003

Diego I. Pedro − *George & Josephine Butler Polymer Research Laboratory, Center for Macromolecular Science & Engineering, Department of Chemistry, University of Florida, Gainesville, Florida 32611-7200, United States*

W. Gregory Sawyer − *George & Josephine Butler Polymer Research Laboratory, Center for Macromolecular Science & Engineering, Department of Chemistry, University of Florida, Gainesville, Florida 32611-7200, United States;* orcid.org/0000-0002-4461-7227

Complete contact information is available at: https://pubs.acs.org/10.1021/acs.macromol.2c01239

Notes

The authors declare no competing financial interest.

■ ACKNOWLEDGMENTS

This work was supported in part by Alcon Research, LLC. This work was supported in part by the National Science Foundation (DMR-1904631) and the DoD through the ARO (W911NF-17-1-0326). Dr. Julia Rho assisted through many fruitful scientific discussions.

■ REFERENCES

(1) Jasinski, F.; Zetterlund, P. B.; Braun, A. M.; Chemtob, A. Photopolymerization in Dispersed Systems. *Prog. Polym. Sci.* **2018**, *84*, 47−88.

(2) Dinsmore, R. P. Synthetic Rubber and Method of Making It. US 1,732,795 A, October 22, 1929.

(3) Odian, G. Emulsion Polymerization. In *Principles of Polymerization*; McGraw-Hill, Inc. 1970; pp. 279−300.

(4) Khan, M.; Guimarães, T. R.; Zhou, D.; Moad, G.; Perrier, S.; Zetterlund, P. B. Exploitation of Compartmentalization in RAFT Miniemulsion Polymerization to Increase the Degree of Livingness. *J. Polym. Sci., Part A: Polym. Chem.* **2019**, *57*, 1938−1946.

(5) Touve, M. A.; Figg, C. A.; Wright, D. B.; Park, C.; Cantlon, J.; Sumerlin, B. S.; Gianneschi, N. C. Polymerization-Induced Self-Assembly of Micelles Observed by Liquid Cell Transmission Electron Microscopy. *ACS Cent. Sci.* **2018**, *4*, 543−547.

(6) Figg, C. A.; Simula, A.; Gebre, K. A.; Tucker, B. S.; Haddleton, D. M.; Sumerlin, B. S. Polymerization-Induced Thermal Self-Assembly (PITSA). *Chem. Sci.* **2015**, *6*, 1230−1236.

(7) Tan, J.; Sun, H.; Yu, M.; Sumerlin, B. S.; Zhang, L. Photo-PISA: Shedding Light on Polymerization-Induced Self-Assembly. *ACS Macro Lett.* **2015**, *4*, 1249−1253.

(8) O'Bryan, C. S.; Kabb, C. P.; Sumerlin, B. S.; Angelini, T. E. Jammed Polyelectrolyte Microgels for 3D Cell Culture Applications: Rheological Behavior with Added Salts. *ACS Appl. Bio Mater.* **2019**, *2*, 1509−1517.

(9) Zetterlund, P. B.; Kagawa, Y.; Okubo, M. Controlled/Living Radical Polymerization in Dispersed Systems. *Chem. Rev.* **2008**, *108*, 3747−3794.

(10) Turro, N. J.; Chow, M.-F.; Chung, C.-J.; Tung, C.-H. An Efficient, High Conversion Photoinduced Emulsion Polymerization. Magnetic Field Effects on Polymerization Efficiency and Polymer Molecular Weight. *J. Am. Chem. Soc.* **1980**, *102*, 7391−7393.

(11) Bianchi, J. P.; Price, F. P.; Zimm, B. H. "Monodisperse" Polystyrene. *J. Polym. Sci.* **1957**, *25*, 27−38.

(12) Tobita, H. Effect of Small Reaction Locus in Free-Radical Polymerization: Conventional and Reversible-Deactivation Radical Polymerization. *Polymer* **2016**, DOI: 10.3390/polym8040155.

(13) Khan, M.; Guimarães, T. R.; Choong, K.; Moad, G.; Perrier, S.; Zetterlund, P. B. RAFT Emulsion Polymerization for (Multi)Block Copolymer Synthesis: Overcoming the Constraints of Monomer Order. *Macromolecules* **2021**, *54*, 736−746.

(14) Richardson, R. A. E.; Guimarães, T. R.; Khan, M.; Moad, G.; Zetterlund, P. B.; Perrier, S. Low-Dispersity Polymers in Ab Initio Emulsion Polymerization: Improved MacroRAFT Agent Performance in Heterogeneous Media. *Macromolecules* **2020**, *53*, 7672−7683.

(15) Rho, J. Y.; Scheutz, G. M.; Häkkinen, S.; Garrison, J. B.; Song, Q.; Yang, J.; Richardson, R.; Perrier, S.; Sumerlin, B. S. In Situ Monitoring of PISA Morphologies. *Polym. Chem.* **2021**, *12*, 3947−3952.

(16) Scheutz, G. M.; Touve, M. A.; Carlini, A. S.; Garrison, J. B.; Gnanasekaran, K.; Sumerlin, B. S.; Gianneschi, N. C. Probing Thermoresponsive Polymerization-Induced Self-Assembly with Variable-Temperature Liquid-Cell Transmission Electron Microscopy. *Matter* **2021**, *4*, 722−736.

(17) Qi, G.; Jones, C. W.; Schork, F. J. RAFT Inverse Miniemulsion Polymerization of Acrylamide. *Macromol. Rapid Commun.* **2007**, *28*, 1010−1016.

(18) Ferguson, C. J.; Hughes, R. J.; Nguyen, D.; Pham, B. T. T.; Gilbert, R. G.; Serelis, A. K.; Such, C. H.; Hawkett, B. S. Ab Initio

Emulsion Polymerization by RAFT-Controlled Self-Assembly. *Macromolecules* **2005**, *38*, 2191−2204.
(19) Ferguson, C. J.; Hughes, R. J.; Pham, B. T. T.; Hawkett, B. S.; Gilbert, R. G.; Serelis, A. K.; Such, C. H. Effective Ab Initio Emulsion Polymerization under RAFT Control. *Macromolecules* **2002**, *35*, 9243−9245.
(20) Simms, R. W.; Cunningham, M. F. High Molecular Weight Poly(Butyl Methacrylate) by Reverse Atom Transfer Radical Polymerization in Miniemulsion Initiated by a Redox System. *Macromolecules* **2007**, *40*, 860−866.
(21) Asua, J. M. Miniemulsion Polymerization. *Progress in Polymer Science (Oxford)*. Elsevier Ltd 2002, pp. 1283−1346.
(22) Oh, J. K.; Tang, C.; Gao, H.; Tsarevsky, N. V.; Matyjaszewski, K. Inverse Miniemulsion ATRP: A New Method for Synthesis and Functionalization of Well-Defined Water-Soluble/Cross-Linked Polymeric Particles. *J. Am. Chem. Soc.* **2006**, *128*, 5578−5584.
(23) Qi, G.; Eleazer, B.; Jones, W. C.; Joseph Schork, F. Mechanistic Aspects of Sterically Stabilized Controlled Radical Inverse Miniemulsion Polymerization. *Macromolecules* **2009**, *42*, 3906−3916.
(24) Zetterlund, P. B.; Okubo, M. Compartmentalization in Nitroxide-Mediated Radical Polymerization in Dispersed Systems. *Macromolecules* **2006**, *39*, 8959−8967.
(25) Tonnar, J.; Pouget, E.; Lacroix-Desmazes, P.; Boutevin, B. Synthesis of Poly(Vinyl Acetate)-Block-Poly(Dimethylsiloxane)-Block-Poly(Vinyl Acetate) Copolymers by Iodine Transfer Photopolymerization in Miniemulsion. *Macromol. Symp.* **2009**, *281*, 20−30.
(26) Fan, W.; Tosaka, M.; Yamago, S.; Cunningham, M. F. Living Ab Initio Emulsion Polymerization of Methyl Methacrylate in Water Using a Water-Soluble Organotellurium Chain Transfer Agent under Thermal and Photochemical Conditions. *Angew. Chem., Int. Ed.* **2018**, *57*, 962−966.
(27) Detrembleur, C.; Debuigne, A.; Bryaskova, R.; Charleux, B.; Jérôme, R. Cobalt-Mediated Radical Polymerization of Vinyl Acetate in Miniemulsion: Very Fast Formation of Stable Poly(Vinyl Acetate) Latexes at Low Temperature. *Macromol. Rapid Commun.* **2006**, *27*, 37−41.
(28) Truong, N. P.; Dussert, M. V.; Whittaker, M. R.; Quinn, J. F.; Davis, T. P. Rapid Synthesis of Ultrahigh Molecular Weight and Low Polydispersity Polystyrene Diblock Copolymers by RAFT-Mediated Emulsion Polymerization. *Polym. Chem.* **2015**, *6*, 3865−3874.
(29) Li, S.; Han, G.; Zhang, W. Photoregulated Reversible Addition−Fragmentation Chain Transfer (RAFT) Polymerization. *Polym. Chem.* **2020**, *11*, 1830−1844.
(30) Nicholas Carmean, R.; Sims, B. M.; Adrian Figg, C.; Hurst, J. P.; Patterson, P. J.; Sumerlin, S. B. Ultrahigh Molecular Weight Hydrophobic Acrylic and Styrenic Polymers through Organic-Phase Photoiniferter-Mediated Polymerization. *ACS Macro Lett.* **2020**, *9*, 613−618.
(31) Carmean, R. N.; Becker, T. E.; Sims, M. B.; Sumerlin, B. S. Ultra-High Molecular Weights via Aqueous Reversible-Deactivation Radical Polymerization. *Chem* **2017**, *2*, 93−101.
(32) Percec, V.; Guliashvili, T.; Ladislaw, J. S.; Wistrand, A.; Stjerndahl, A.; Sienkowska, M. J.; Monteiro, M. J.; Sahoo, S. Ultrafast Synthesis of Ultrahigh Molar Mass Polymers by Metal-Catalyzed Living Radical Polymerization of Acrylates, Methacrylates, and Vinyl Chloride Mediated by SET at 25 °C. *J. Am. Chem. Soc.* **2006**, *128*, 14156−14165.
(33) Nicolaÿ, R.; Kwak, Y.; Matyjaszewski, K. A Green Route to Well-Defined High-Molecular-Weight (Co)Polymers Using ARGET ATRP with Alkyl Pseudohalides and Copper Catalysis. *Angew. Chem., Int. Ed.* **2010**, *49*, 541−544.
(34) Read, E.; Guinaudeau, A.; James Wilson, D.; Cadix, A.; Violleau, F.; Destarac, M. Low Temperature RAFT/MADIX Gel Polymerisation: Access to Controlled Ultra-High Molar Mass Polyacrylamides. *Polym. Chem.* **2014**, *5*, 2202−2207.
(35) Hayashi, M.; Noro, A.; Matsushita, Y. Highly Extensible Supramolecular Elastomers with Large Stress Generation Capability Originating from Multiple Hydrogen Bonds on the Long Soft Network Strands. *Macromol. Rapid Commun.* **2016**, *37*, 678−684.
(36) Liu, Z.; Lv, Y.; An, Z. Enzymatic Cascade Catalysis for the Synthesis of Multiblock and Ultrahigh-Molecular-Weight Polymers with Oxygen Tolerance. *Angew. Chem., Int. Ed.* **2017**, *56*, 13852−13856.
(37) An, Z. 100th Anniversary of Macromolecular Science Viewpoint: Achieving Ultrahigh Molecular Weights with Reversible Deactivation Radical Polymerization. *ACS Macro Lett.* **2020**, *9*, 350−357.
(38) Rzayev, J.; Penelle, J. HP-RAFT: A Free-Radical Polymerization Technique for Obtaining Living Polymers of Ultrahigh Molecular Weights. *Angew. Chem., Int. Ed.* **2004**, *43*, 1691−1694.
(39) Otsu, T.; Yoshida, M. Role of Initiator-Transfer Agent-Terminator (Iniferter) in Radical Polymerizations: Polymer Design by Organic Disulfides as Iniferters. *Die Makromol. Chem., Rapid Commun.* **1982**, *3*, 127−132.
(40) Otsu, T. Iniferter Concept and Living Radical Polymerization. *J. Polym. Sci., Part A: Polym. Chem.* **2000**, *38*, 2121−2136.
(41) Thum, M. D.; Wolf, S.; Falvey, D. E. State-Dependent Photochemical and Photophysical Behavior of Dithiolate Ester and Trithiocarbonate Reversible Addition−Fragmentation Chain Transfer Polymerization Agents. *J. Phys. Chem. A* **2020**, *124*, 4211−4222.
(42) McKenzie, T. G.; Fu, Q.; Wong, E. H. H.; Dunstan, D. E.; Qiao, G. G. Visible Light Mediated Controlled Radical Polymerization in the Absence of Exogenous Radical Sources or Catalysts. *Macromolecules* **2015**, *48*, 3864−3872.
(43) Otsu, T.; Matsunaga, T.; Kuriyama, A.; Yoshioka, M. Living Radical Polymerization through the Use of Iniferters: Controlled Synthesis of Polymers. *Eur. Polym. J.* **1989**, *25*, 643−650.
(44) You, Y.-Z.; Hong, C.-Y.; Bai, R.-K.; Pan, C.-Y.; Wang, J. Photo-Initiated Living Free Radical Polymerization in the Presence of Dibenzyl Trithiocarbonate. *Macromol. Chem. Phys.* **2002**, *203*, 477−483.
(45) Xu, J.; Shanmugam, S.; Corrigan, N.; Boyer, C. Catalyst-Free Visible Light-Induced RAFT Photopolymerization. In *Controlled Radical Polymerization: Mechanisms*; ACS Symposium Series; American Chemical Society, 2015; Vol. *1187*, pp. 13−247.
(46) Liu, Y.; Santa Chalarca, C. F.; Nicholas Carmean, R.; Olson, R. A.; Madinya, J.; Sumerlin, B. S.; Sing, C. E.; Emrick, T.; Perry, S. L. Effect of Polymer Chemistry on the Linear Viscoelasticity of Complex Coacervates. *Macromolecules* **2020**, 7851−7864.
(47) Carmean, R. N.; Figg, C. A.; Scheutz, G. M.; Kubo, T.; Sumerlin, B. S. Catalyst-Free Photoinduced End-Group Removal of Thiocarbonylthio Functionality. *ACS Macro Lett.* **2017**, *6*, 185−189.
(48) Easterling, C. P.; Xia, Y.; Zhao, J.; Fanucci, G. E.; Sumerlin, B. S. Block Copolymer Sequence Inversion through Photoiniferter Polymerization. *ACS Macro Lett.* **2019**, *8*, 1461−1466.
(49) Quinn, J. F.; Barner, L.; Barner-Kowollik, C.; Rizzardo, E.; Davis, T. P. Reversible Addition−Fragmentation Chain Transfer Polymerization Initiated with Ultraviolet Radiation. *Macromolecules* **2002**, *35*, 7620−7627.
(50) Storey, R. F. Fundamental Aspects of Living Polymerization. In *Fundamentals of Controlled/Living Radical Polymerization*; The Royal Society of Chemistry, 2013; pp. 60−77.
(51) Matyjaszewski, K. Ranking Living Systems. *Macromolecules* **1993**, *26*, 1787−1788.
(52) Shim, S. E.; Shin, Y.; Jun, J. W.; Lee, K.; Jung, H.; Choe, S. Living-Free-Radical Emulsion Photopolymerization of Methyl Methacrylate by a Surface Active Iniferter (Suriniferter). *Macromolecules* **2003**, *36*, 7994−8000.
(53) Zhao, M.; Zhang, H.; Ma, F.; Zhang, Y.; Guo, X.; Zhang, H. Efficient Synthesis of Monodisperse, Highly Crosslinked, and "Living" Functional Polymer Microspheres by the Ambient Temperature Iniferter-Induced "Living" Radical Precipitation Polymerization. *J. Polym. Sci., Part A: Polym. Chem.* **2013**, *51*, 1983−1998.
(54) Li, J.; Zu, B.; Zhang, Y.; Guo, X.; Zhang, H. One-Pot Synthesis of Surface-Functionalized Molecularly Imprinted Polymer Microspheres by Iniferter-Induced "Living" Radical Precipitation Polymerization. *J. Polym. Sci., Part A: Polym. Chem.* **2010**, *48*, 3217−3228.

https://doi.org/10.1021/acs.macromol.2c01239
Macromolecules 2022, 55, 8451−8460

(55) Kwak, J.; Lacroix-Desmazes, P.; Robin, J. J.; Boutevin, B.; Torres, N. Synthesis of Mono Functional Carboxylic Acid Poly-(Methyl Methacrylate) in Aqueous Medium Using Sur-Iniferter. Application to the Synthesis of Graft Copolymers Polyethylene-g-Poly(Methyl Methacrylate) and the Compatibilization of LDPE/PVDF Blends. *Polymer* **2003**, *44*, 5119−5130.
(56) Mapas, J. K. D.; Thomay, T.; Cartwright, A. N.; Ilavsky, J.; Rzayev, J. Ultrahigh Molecular Weight Linear Block Copolymers: Rapid Access by Reversible-Deactivation Radical Polymerization and Self-Assembly into Large Domain Nanostructures. *Macromolecules* **2016**, *49*, 3733−3738.
(57) Dao, V. H.; Cameron, N. R.; Saito, K. Synthesis of UHMW Star-Shaped AB Block Copolymers and Their Flocculation Efficiency in High-Ionic-Strength Environments. *Macromolecules* **2019**, *52*, 7613−7624.
(58) Plucinski, A.; Pavlovic, M.; Schmidt, B. V. K. J. All-Aqueous Multi-Phase Systems and Emulsions Formed via Low-Concentration Ultra-High-Molar Mass Polyacrylamides. *Macromolecules* **2021**, *54*, 5366−5375.
(59) Sun, J. Z.; Erickson, M. C. E.; Parr, J. W. Refractive Index Matching and Clear Emulsions. *Int. J. Cosmet. Sci.* **2005**, *56*, 253−265.
(60) Jung, K.; Boyer, C.; Zetterlund, P. B. RAFT Iniferter Polymerization in Miniemulsion Using Visible Light. *Polym. Chem.* **2017**, *8*, 3965−3970.
(61) Guimarães, T. R.; Bong, Y. L.; Thompson, S. W.; Moad, G.; Perrier, S.; Zetterlund, P. B. Polymerization-Induced Self-Assembly via RAFT in Emulsion: Effect of Z-Group on the Nucleation Step. *Polym. Chem.* **2021**, *12*, 122−133.
(62) Thomas, D. B.; Convertine, A. J.; Hester, R. D.; Lowe, A. B.; McCormick, C. L. Hydrolytic Susceptibility of Dithioester Chain Transfer Agents and Implications in Aqueous RAFT Polymerizations. *Macromolecules* **2004**, *37*, 1735−1741.
(63) Fuchs, A. V.; Thurecht, K. J. Stability of Trithiocarbonate RAFT Agents Containing Both a Cyano and a Carboxylic Acid Functional Group. *ACS Macro Lett.* **2017**, *6*, 287−291.
(64) Zetterlund, P. B.; D'hooge, D. R. The Nanoreactor Concept: Kinetic Features of Compartmentalization in Dispersed Phase Polymerization. *Macromolecules* **2019**, *52*, 7963−7976.

https://doi.org/10.1021/acs.macromol.2c01239
Macromolecules 2022, 55, 8451−8460